

Hydrogen Transportation and Distributed Energy Systems Seismic Risk Assessment for Cascadia Subduction Zone Airport Facilities

August 2025

Arun Veeramany*
Melissa S. Louie+
Brooke M. Marten*
Marina Miletic+
Bhavya Mamnani*
Brian D. Ehrhart+

*Pacific Northwest National Laboratory

+Sandia National Laboratories

DISCLAIMER

This report was prepared as an account of work sponsored by an agency of the United States Government. Neither the United States Government nor any agency thereof, nor Battelle Memorial Institute, nor any of their employees, makes **any warranty, express or implied, or assumes any legal liability or responsibility for the accuracy, completeness, or usefulness of any information, apparatus, product, or process disclosed, or represents that its use would not infringe privately owned rights.** Reference herein to any specific commercial product, process, or service by trade name, trademark, manufacturer, or otherwise does not necessarily constitute or imply its endorsement, recommendation, or favoring by the United States Government or any agency thereof, or Battelle Memorial Institute. The views and opinions of authors expressed herein do not necessarily state or reflect those of the United States Government or any agency thereof.

PACIFIC NORTHWEST NATIONAL LABORATORY

operated by

BATTELLE

for the

UNITED STATES DEPARTMENT OF ENERGY

under Contract DE-AC05-76RL01830

Printed in the United States of America

Available to DOE and DOE contractors from
the Office of Scientific and Technical Information,
P.O. Box 62, Oak Ridge, TN 37831-0062

www.osti.gov

ph: (865) 576-8401

fox: (865) 576-5728

email: reports@osti.gov

Available to the public from the National Technical Information Service
5301 Shawnee Rd., Alexandria, VA 22312

ph: (800) 553-NTIS (6847)

or (703) 605-6000

email: info@ntis.gov

Online ordering: <http://www.ntis.gov>

Hydrogen Transportation and Distributed Energy Systems Seismic Risk Assessment for Cascadia Subduction Zone Airport Facilities

August 2025

Arun Veeramany*
Melissa S. Louie+
Brooke M. Marten*
Marina Miletic+
Bhavya Mamnani*
Brian D. Ehrhart+

Prepared for
the U.S. Department of Energy
under Contract DE-AC05-76RL01830

*Pacific Northwest National Laboratory
+Sandia National Laboratories

Pacific Northwest National Laboratory
Richland, Washington 99354

Executive Summary

Portland International Airport in Oregon is exploring operating a fleet of 28 fuel cell electric buses to support airport operations and possibly provide backup power during outages. In this report, we evaluate the risk of hydrogen deployment at an airport considering the potential for seismic activity. We present a seismic risk assessment for pressurized piping for a generic hydrogen refueling station at the airport. Only pressurized piping was considered in the risk analysis because of its vulnerability and availability of fragility information unlike the other components. Seismic capacity of other components should be included as more information becomes available.

To characterize the seismic hazard, we considered the initiating event frequency of a Cascadia Subduction Zone earthquake event based on data from the literature. Seismic stressors that translate to the site from an earthquake event are expressed as peak ground acceleration. Site disturbance is characterized as a function of soil conditions, represented by different shear wave velocity values, which affect how seismic waves propagate and impact structures. Pipe fragility curves as a function of seismic capacity were used to correlate ground acceleration and failure probability. These fragility characteristics were combined with site-specific soil conditions to calculate the probability of pipe rupture during a seismic event. It should be noted that multiple simultaneous failures due to an earthquake event as a common cause are not considered. Some epistemic uncertainties such as self-exciting shocks, aftershocks, and the time variant nature of the ground motion are not considered either.

We performed a quantitative risk assessment to determine annual leak frequencies and associated location-specific individual fatality risks for piping under seismic and normal (non-seismic) conditions. Fatality risk analysis was performed based on distance from the leak source, resulting in spatial risk contours which can inform facility layout decisions.

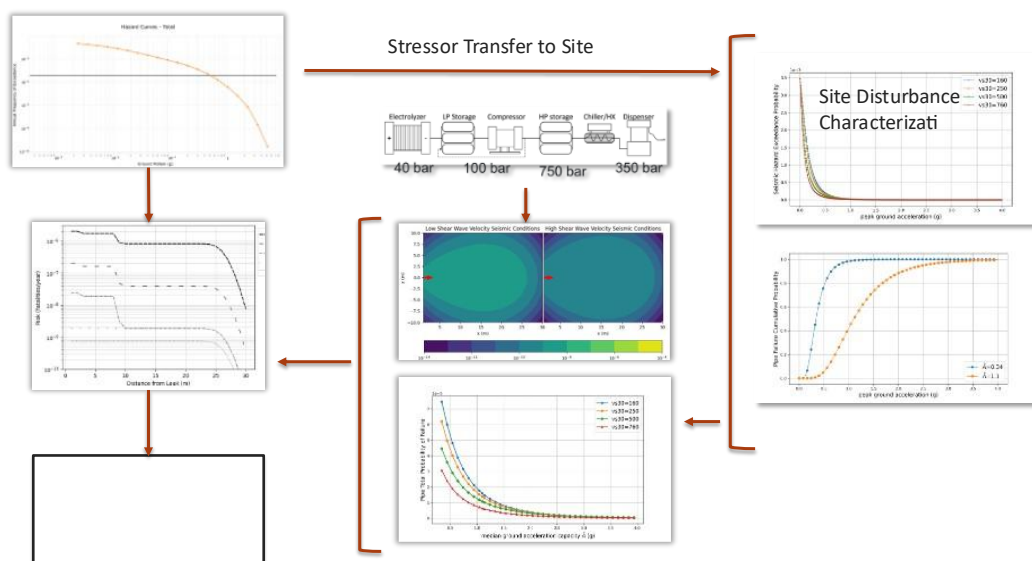


Figure ES-1. Seismic risk assessment methodology for a hydrogen fueling infrastructure at Portland International Airport.

Using site-specific seismic hazard assessments and quantitative risk analysis, we estimated that the seismic condition leak frequency for a full-bore leak for pipes is generally at least an order of magnitude lower than full-bore leak frequencies for pipes under normal, non-seismic-specific operational conditions. Our analysis shows that soil conditions may cause seismic risk to increase, although this risk remains low overall compared to normal non-seismic-specific operational risk. Fatality risk decreases significantly with distance from the leak point across all scenarios, with a dramatic decrease occurring further than 25 m from the leak. Under normal, non-seismic-specific conditions, the median risk for full-bore pipe leaks is around 10^{-8} to 10^{-7} fatalities/year near the source, and the risk decreases with distance. Under only seismic conditions, the risk for full-bore pipe leaks is at least one order of magnitude lower, with approximately 10^{-10} to 10^{-9} fatalities/year for high shear wave velocity soil conditions (stiffer soils). This risk analysis suggests that while seismic risk should not be ignored, it is not as significant as the risk under normal non-seismic conditions for full-bore leaks. This is likely due to an ensemble of conditions: normal, non-seismic specific risk values inherently encompassing some seismic risk components, in addition to other leak-inducing factors that may include component wear or corrosion, other natural disasters, and damage from misuse of the system. While this analysis is somewhat an indicator of the contributions of seismic risk to overall risk of a hydrogen storage and dispensing system, its sole inclusion of full-bore pipe leaks, and exclusion of other components and leak sizes due to lack of data, may mean that the risk trends shown are not necessarily indicative of actual risk for the entire system. Our focus on low-frequency, high consequence full-bore leaks in this study does not account for how smaller, partial leaks can also occur and impact the overall risk.

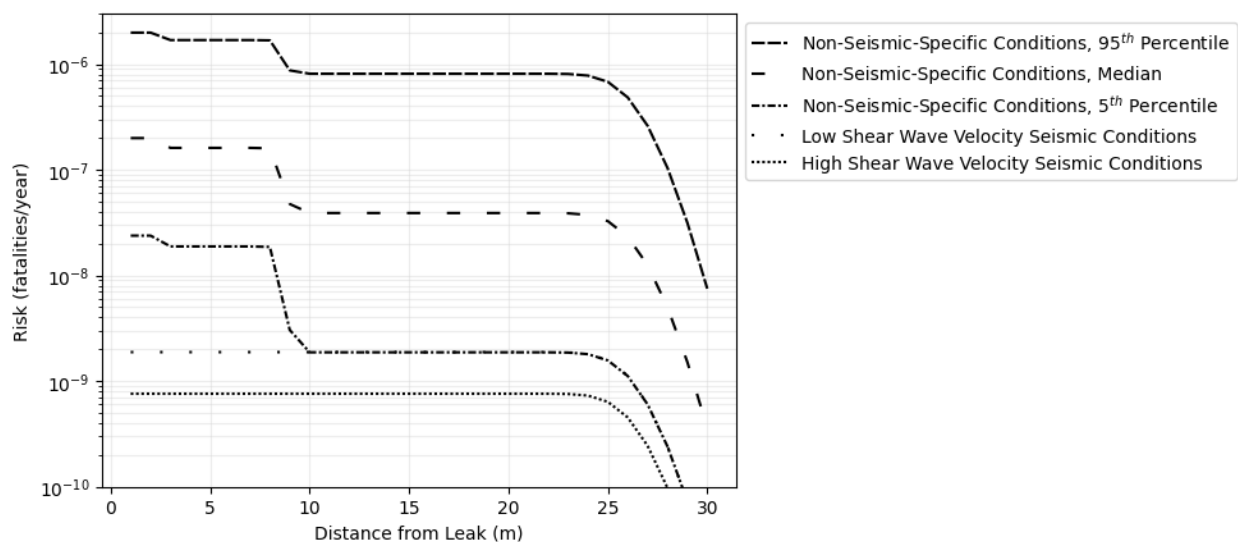


Figure ES-2. Annual individual risk for full bore leaks based on distance from the leak.

Robust design and operational protocols can enhance the resilience of hydrogen infrastructure and minimize overall risk. Appropriate pipe material selection, placement, thickness, anchoring, and orientation may lower risk of leaks during seismic events. Also, seismic-resistant design of piping networks and trenching may reduce the likelihood of failure. Regular inspection and maintenance protocols, appropriate emergency response procedures, and training are important for ensuring operating safety and properly maintaining equipment.

Acronyms and Abbreviations

CSZ	Cascadia Subduction Zone
HFTO	Hydrogen and Fuel Cell Technologies Office
HyRAM+	Hydrogen Plus Other Alternative Fuels Risk Assessment Models
PDX	Portland International Airport
USGS	U.S. Geological Survey
VCT	volume control tank

Contents

Executive Summaryiii

Acronyms and Abbreviations v

1.0 Introduction 1

2.0 Seismic Hazard Assessment 2

3.0 Seismic Risk Assessment 5

 3.1 Assumptions..... 5

 3.2 Estimation of the Probability of Total Pipe Failure under Seismic
 Conditions 6

 3.3 Quantitative Risk Assessment Comparison under Seismic and Normal
 Conditions 8

4.0 Possible Mitigation Approaches 13

5.0 Conclusion 14

6.0 References 16

Appendix A – Supplemental Data A-1

Figures

Figure 1.	Annual rate of exceedance hazard curve for ground conditions typical at Portland International Airport assuming soft soil conditions ($V_{S30} = 210$ m/s). Source: USGS (2018b).....	2
Figure 2.	Seismic disaggregation of the Cascadia seismic interface for Portland International Airport assuming a shear wave velocity $V_{S30} = 210$ m/s. Epsilon (ϵ) corresponds to the deviation of the observed ground motion from the median. Closest Distance corresponds to R (the deviation of the observed ground motion from the median). Chart adapted from USGS (2018a).	3
Figure 3.	V_{S30} soil condition values for regions around Portland International Airport. Source: McPhillips et al. (2020).	4
Figure 4.	Probability of failure of a hydrogen pipe given the ground motion at Portland International Airport due to seismic hazard and hydrogen piping fragility. Cascadia seismic hazard curve (upper left), Pipe fragility curve for pipe median ground acceleration capacities (\hat{A}) of 0.34g and 1.1g (lower left), Probability of total pipe failure based on V_{S30} soil conditions for different pipe median ground acceleration capacities (\hat{A}) (right). The table shows the probability of Total Pipe Failure per seismic event, based on \hat{A} and V_{S30}	7
Figure 5.	Two-dimensional contour plot of annual individual risks (birds-eye view) for full bore leaks. The red arrow indicates the leak origin and direction; it is not indicative of the size of the leak. Top: 5th, median, and 95th percentile leak frequency distributions for normal, non-seismic-specific conditions. Bottom left: $V_{S30} = 160$ m/s seismic conditions. Bottom right: $V_{S30} = 760$ m/s seismic conditions.	10
Figure 6.	Annual individual risk for full bore leaks based on distance from the leak.	11

Tables

Table 1.	Probability or frequency of total pipe failure under seismic conditions, based on shear wave velocity, seismic event frequency, and length of pipe, assuming a pipe median ground acceleration capacity (\hat{A}) of 1.1g.	8
Table 2.	Annual leak frequencies per meter of pipe for normal, non-seismic-specific as well as seismic conditions, assuming a pipe median ground acceleration capacity (\hat{A}) of 1.1 g. Percentages refer to leak sizes based on the percentage of the cross-sectional area of the pipe. * = Data not available.	9

1.0 Introduction

Oregon has a significant risk of experiencing a greater than 9.0M earthquake within the next 50 years. Because federal and state agencies are interested in Portland International Airport (PDX) as a key response center for Multnomah County (2023), ensuring that PDX can remain operational is critical to initial response. During such events, as much of 2 weeks of emergency operations may be required. This project examined the seismic risk for deployment of hydrogen during such events and how this may aid in PDX's emergency response goals.

This seismic analysis includes a PDX site-specific assessment of the probability for an earthquake to lead to a full-bore leak pipe failure from a hypothetical hydrogen fuel cell bus refueling piping system, and other metrics such as fatality risk due to such a rupture. Because PDX already is investing in resilient runway infrastructure (NIBS 2021), informing the next stages of a resilient transportation system will be valuable in planning the operational functions necessary after a seismic event to serve Oregon's Willamette Valley and southwest Washington.

2.0 Seismic Hazard Assessment

The PDX region is vulnerable to intraslab, subduction, and fault events. Intraslab seismic events occur within a continental tectonic plate, subduction zone earthquakes occur at the interface between continental and oceanic plates, and fault line events occur at the interface of two tectonic plates. Higher ground motion has a lower probability of occurrence relative to lower (or deeper) ground motion. Notably, even though an earthquake may have a smaller magnitude on the Richter scale, its associated ground motion could be relatively higher compared to that of a higher magnitude earthquake. This study focuses on the impact of Cascadia Subduction Zone (CSZ) earthquakes on hypothetical hydrogen infrastructure at an airport facility.

A hazard curve shown in Figure 1 provides critical insights into seismic risk at the PDX site. The graph is derived from the U.S. Geological Survey (USGS) 2023 National Seismic Hazard Model for the coterminous United States and accounts for intraslab, subduction, and fault events (Petersen et al. 2024). The curve is based on a site class representative of soft soil conditions reflecting high amplification potential, a return period of 2,475 years (2% probability of exceedance in 50 years), and annual frequency of exceedance plotted against ground motion levels (measured in "g," the fraction of Earth's gravitational acceleration).

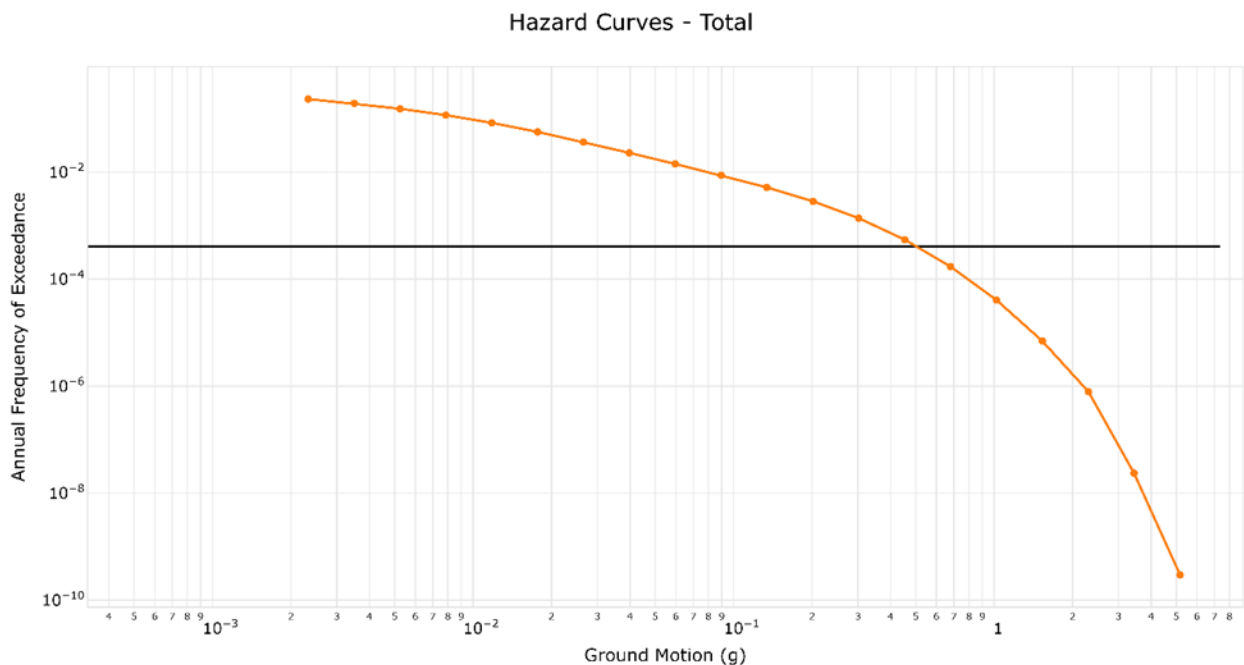


Figure 1. Annual rate of exceedance hazard curve for ground conditions typical at Portland International Airport assuming soft soil conditions ($V_{s30} = 210$ m/s). Source: USGS (2018b).

This hazard exceedance curve characterizes the likelihood of varying ground motion intensities and is essential for risk-informed design decisions, particularly in earthquake-prone areas. The ground motion values span a wide range, from less than 0.01 g to approximately 5 g. The curve includes higher exceedance frequencies (10^{-2} per year) for low ground motion levels and rapidly declines for increasing ground motions, reaching extremely low exceedance frequencies (below 10^{-6} per year). A horizontal line is drawn at an annual exceedance frequency of approximately 5×10^{-4} per year. This is a benchmark commonly used in seismic design, corresponding to a

2,475-year return period. At an exceedance frequency of 10^{-4} per year, the corresponding ground motion level is around 0.7 g. For extreme ground motion intensities (e.g., 4–5 g), the exceedance frequencies drop significantly, indicating these intensities are improbable according to this model.

Even though seismic activity exceeding 0.7 g (close to the 10^{-4} exceedance benchmark) are far less likely, such ground motions can have devastating effects on infrastructure, underscoring the need for earthquake-resistant design. The model accounts for both moderate-magnitude crustal events and rare, large-magnitude CSZ earthquakes, which dominate the hazard for high-intensity shaking.

The rest of this section provides an interpretation of the USGS Earthquake Hazard Toolbox disaggregation report shown in Figure 2 for the Portland, Oregon, region.

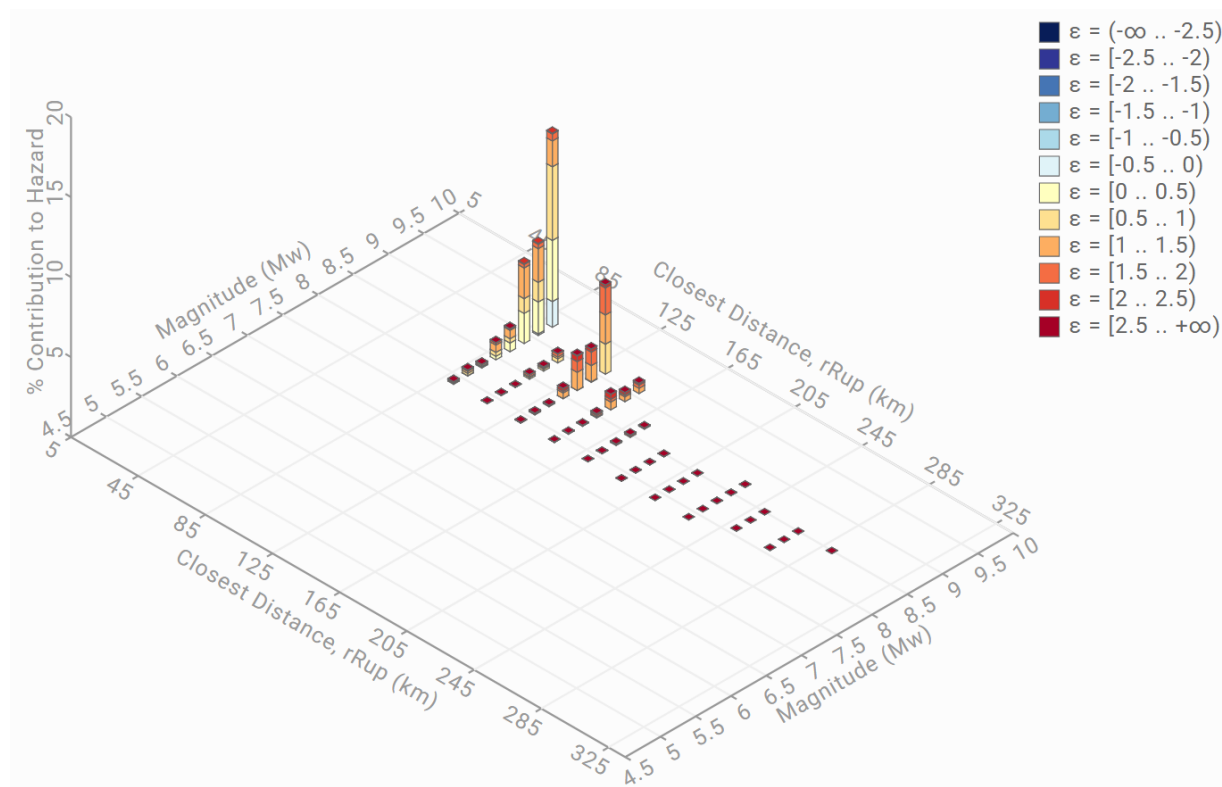


Figure 2. Seismic disaggregation of the Cascadia seismic interface for Portland International Airport assuming a shear wave velocity $V_{S30} = 210$ m/s. Epsilon (ϵ) corresponds to the deviation of the observed ground motion from the median. Closest Distance corresponds to R (the deviation of the observed ground motion from the median). Chart adapted from USGS (2018a).

The largest contribution to hazard comes from events with magnitude (M_w) of 9.28, distance (R) of 83.64 km and an epsilon (ϵ) of 0.59σ which indicates deviation of the observed ground motion from the median. This specific scenario contributes 12% to the total hazard. The site faces multiple significant seismic threats including large magnitude (8.5–9.5 M_w) subduction events from the CSZ. The soft soil conditions could amplify ground motions, which is reflected in the hazard calculations. The high epsilon values (average deviation of 0.98σ) suggest that rare, larger-than-median ground motions contribute significantly to the hazard within this return period.

V_{S30} corresponds to the shear wave velocity (i.e., how quickly a shear wave moves) through soil 30 m under the earth's surface. A higher value, such as a V_{S30} equal to or greater than 760 m/s, indicates a stiffer soil and better resistance to earthquake movement. A lower value, such as a V_{S30} equal to or less than 180 m/s, corresponds to softer soil which can amplify seismic waves. The Portland (PDX) region exhibits a range of V_{S30} values, indicating varying soil stiffness across the area as seen in Figure 3.



Figure 3. V_{S30} soil condition values for regions around Portland International Airport.
Source: McPhillips et al. (2020).

The map shows that regions closer to the Columbia River and areas within Portland itself generally have lower V_{S30} values (ranging from less than 180 m/s to 300 m/s), suggesting softer soil conditions. In contrast, areas further east and south, particularly towards the foothills and away from major river systems, tend to have higher V_{S30} values (ranging from 360 m/s to greater than 760 m/s), indicating stiffer soil profiles. This spatial variation in V_{S30} is crucial for seismic hazard assessment, as softer soils amplify ground motions during earthquakes, potentially leading to increased damage to structures in those areas. This analysis may help support PDX in their risk-informed placement of support equipment.

3.0 Seismic Risk Assessment

3.1 Assumptions

Assessing seismic risk for hydrogen fuel cell electric buses used at airport facilities can be complex and involve identifying and quantifying many different types and sources of failure. The leak frequency and failure data needed to perform a thorough seismic risk assessment is often unavailable since seismic events occur so infrequently, making extensive risk assessment more challenging. The work presented here does not provide a comprehensive quantitative risk assessment under seismic conditions. Instead, we have focused this seismic risk assessment on quantifying the risk and associated hazards of hydrogen pipe rupture, largely because of the availability of seismic risk data for pipes carrying pressurized hydrogen. Pipes are relevant components since they are critical to refueling and contain hydrogen under a range of pressures while spanning large outdoor distances. Quantifying and comparing the risk of pipe rupture for a hydrogen refueling station under normal and seismic conditions aids in understanding the possible effects of an earthquake on such a system. However, if hydrogen fuel cell buses are refueled using mobile tanks delivered on site, the risks outlined here are less relevant since there would be no stationary refueling station with hundreds of feet of piping on-site.

The nuclear industry has collected relevant data and performed seismic risk assessments for various power plant components, including pressurized hydrogen pipes. Pipe failure data is presented in NUREG/CR-5759, a document which provides risk assessment information on the use of hydrogen at nuclear facilities (NRC 1993). The data presented in NUREG/CR-5759 are based on plant visits conducted at 15 pressurized water reactor sites. For pressurized water reactors, the volume control tank (VCT) is pressurized with hydrogen gas delivered from the hydrogen gas system, which is supplied in pipes. Hydrogen is pumped into the VCT to react with oxygen from the coolant (borated water) to prevent corrosion. It is this NUREG/CR-5759 hydrogen pipe failure risk data that is applied in part in this current work to help determine the probability of pipe failure under seismic conditions.

As outlined in NUREG/CR-5759, there was large design variability observed among VCT hydrogen gas systems at different plant sites, contributing to the variability of failure risk (NRC 1993). The largest variability was that of the VCT hydrogen supply pipe length inside auxiliary buildings at different plants, which ranged from 15–300 ft (4.6–91 m). For this current risk analysis, we assumed that the probability of total pipe failure was based on a pipe length of 15 ft (4.6 m), as this would provide the most conservative assessment. Some other differences in VCT hydrogen gas system designs included pipe diameter (specified as less than 3 inches [7.6 centimeters]), the degree to which pipes were anchored and welded for seismic conditions, their materials of construction (such as carbon steel versus stainless), sleeved versus un-sleeved pipes, and the presence or absence of check valves. These factors, especially pipe length and diameter, all contribute to variability in failure risk, and this is reflected in the seismic risk numbers presented here, since they are based on the probability of pipe failure of an aggregate of many different pipe configurations and designs at different facilities.

Since leak frequencies from seismic activity were only available for pipes, this risk assessment only included the piping network feeding the PDX bus refueling station dispenser facility, which was specified as a network of 50 m of piping (Louie et al. n.d.). The seismic activity was assumed to only cause full-bore, 100% leaks, i.e., what would be expected for a total pipe failure or disconnection. There could be seismic impact on non-piping components as well, and

because of a lack of leak frequency data for these components, we were unable to estimate their performance under seismic conditions. We feel that focusing on pipe failure emphasizes an important and potentially vulnerable aspect of the system.

In this work, to calculate pipe rupture frequency under seismic conditions, we used a site-specific seismic hazard exceedance curve for a Cascadia seismic rupture source together with pipe failure probabilities from NUREG/CR-5759 to estimate the probability of total pipe failure per seismic event (NRC 1993). While the piping fragility is anticipated to be the same for any infrastructure other than PDX assuming the same setup, the hazard exceedance curve will be different given the seismic sources. To calculate the pipe rupture frequency under normal, non-seismic-specific conditions, we used leak frequency data from the risk assessment software toolkit Hydrogen Plus Other Alternative Fuels Risk Assessment Models (HyRAM+) v5.1.1 (Ehrhart et al. 2023). HyRAM+ includes empirically validated models of leaks and other hazardous behavior based on experimental and industrial data and simulations, including normal use and possibly rare events such as earthquakes. The calculation of pipe rupture frequency under seismic conditions is explained in the following section.

3.2 Estimation of the Probability of Total Pipe Failure under Seismic Conditions

The probability of failure of a 316/316L class pipe carrying hydrogen in the nuclear industry depends on seismic ground motion. The seismic capacity (\hat{A}) of a hydrogen pipe referenced from (Simion et al. 1992) is 1.1 g with a logarithmic standard deviation of 0.5 g and a high-confidence low probability of failure (HCLPF) at 0.34 g. The HCLPF value is the ground motion estimate below which the pipe is unlikely to fail. A component fails when its resistance to the stress from earthquake-induced ground motion is inadequate.

To relate the effect of ground motion on a component such as a pipe, a mathematical correlation can be created. The consideration of both the site-specific hazard curve for a Cascadia seismic rupture source and a pipe fragility curve taken together can yield a site-specific probability of pipe failure as a result of an earthquake, as illustrated in Figure 4.

The associated probability for realization of the hazard is represented by P . This probability is a scalar value and is obtained by integrating the product of the hazard curve (representing the stress) and the fragility curve (representing the resistance) as described by (Kennedy 1999):

$$P = \int_0^{\infty} H(s)f(s)ds \quad (1)$$

where s represents peak ground acceleration (g), the hazard exceedance distribution is represented by $H(s)$, and piping fragility is given by pipe density, $f(s)$. The total probability of failure P was estimated for multiple values of shear wave velocity representing soil conditions (V_{S30}) and pipe median peak ground acceleration, \hat{A} , as tabulated in Figure 4.

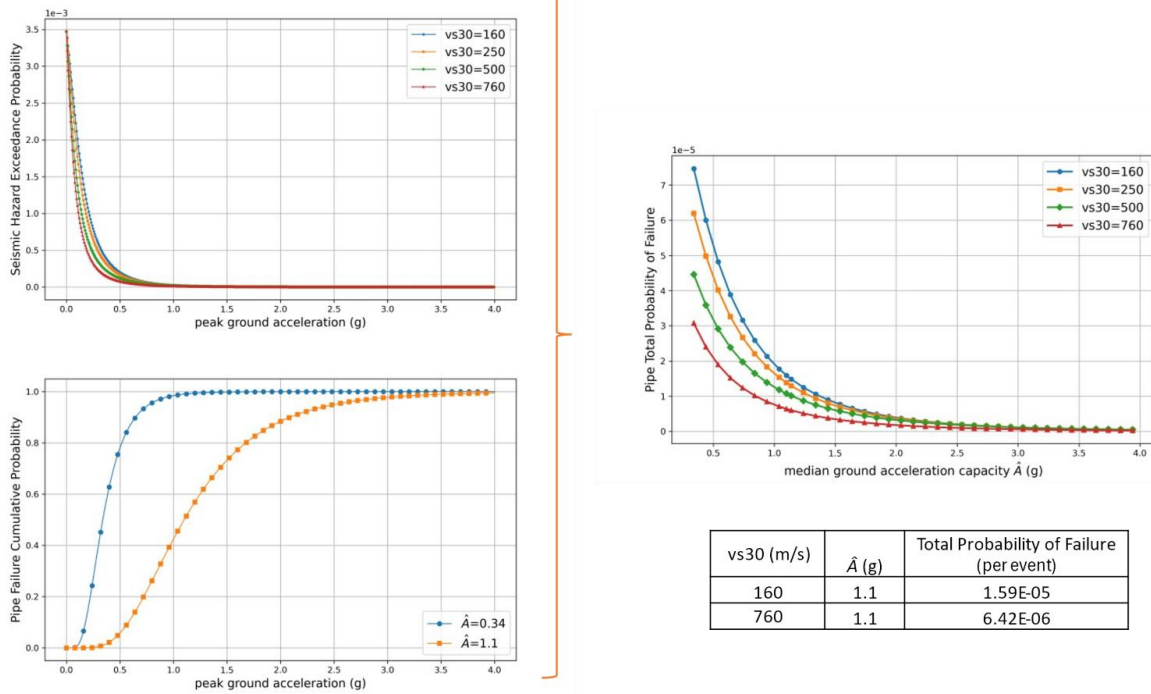


Figure 4. Probability of failure of a hydrogen pipe given the ground motion at Portland International Airport due to seismic hazard and hydrogen piping fragility. Cascadia seismic hazard curve (upper left), Pipe fragility curve for pipe median ground acceleration capacities (\hat{A}) of 0.34g and 1.1g (lower left), Probability of total pipe failure based on V_{S30} soil conditions for different pipe median ground acceleration capacities (\hat{A}) (right). The table shows the probability of Total Pipe Failure per seismic event, based on \hat{A} and V_{S30} .

A lower \hat{A} corresponds to a pipe that cannot withstand as much shaking before failure, compared to a pipe with a higher \hat{A} . Therefore, pipes with a lower \hat{A} have a higher probability of failure for any given peak ground acceleration (g) compared to pipes with a higher \hat{A} . For a given V_{S30} , the pipe's probability of failure decreases because the pipe can withstand greater shaking. As V_{S30} increases, corresponding to stiffer soil, the pipe's probability of failure decreases because there is generally less ground motion transmission to pipes.

The recurrence interval for Cascadia seismic events is about 490 to 550 years (Goldfinger et al. 2003). To calculate the probability of annual pipe failure under seismic conditions, we assumed Cascadia seismic events occur every 490 years, as this would yield more conservative risk estimates. The Probability of Total Pipe Failure per Seismic Event (1.59×10^{-5} for $V_{S30} = 160$ m/s and 6.42×10^{-6} for $V_{S30} = 760$ m/s from Figure 4) is divided by the 490-year frequency value to yield the Frequency of Total Pipe Failure per Year (3.24×10^{-8} for $V_{S30} = 160$ m/s and 1.31×10^{-8} for $V_{S30} = 760$ m/s). As outlined earlier, this frequency assumes a pipe length of 15 ft (4.57 m). To obtain the Frequency of Total Pipe Failure per Year per Meter, the Frequency of Total Pipe Failure per Year was divided by 4.57. These values are shown in Table 1.

Table 1. Probability or frequency of total pipe failure under seismic conditions, based on shear wave velocity, seismic event frequency, and length of pipe, assuming a pipe median ground acceleration capacity (\hat{A}) of 1.1g.

	Probability of Total Pipe Failure per Seismic Event	Frequency of Total Pipe Failure per Year	Frequency of Total Pipe Failure per Year per Meter
$V_{S30} = 160 \text{ m/s}$	1.59×10^{-5}	3.24×10^{-8}	7.10×10^{-9}
$V_{S30} = 760 \text{ m/s}$	6.42×10^{-6}	1.31×10^{-8}	2.87×10^{-9}

The Frequency of Total Pipe Failure per Year per Meter is useful when comparing risk of pipe rupture under seismic vs. normal (non-seismic-specific) conditions, as discussed in the next section.

3.3 Quantitative Risk Assessment Comparison under Seismic and Normal Conditions

A quantitative risk assessment performed using HyRAM+ v5.1.1 (Ehrhart et al. 2023) was used to examine the potential impacts of different seismic effects on individual risk. This assessment methodology couples leak frequencies with ignition probabilities to quantify overall annual frequencies of harmful ignition events such as jet fires and explosions. The magnitude of the consequence from each scenario resulting in an ignition event is then calculated based on consequence-specific metrics for each—heat flux for jet fires and overpressure and impulse for explosions. These physical metrics are used as inputs in selected probit models, which are used to convert the metrics into probabilities of harm to people or infrastructure. In this risk assessment, the hazard of interest was the probability of fatality for a single person at various distances away from a potential leak. That probability was applied with the ignition event frequencies to calculate an individual annual frequency of fatality. The assumed inputs for this risk assessment are shown in Table A-1.

Risks were calculated under three different conditions. The first condition considers normal, non-seismic-specific activity, where default annual leak frequency values from HyRAM+ were used (Ehrhart et al. 2023). The per-component gaseous hydrogen leak frequency data in HyRAM+ is based on generic oil and gas industry data, which means leaks from different sources over time, potentially including seismic activity, are included (Glover et al. 2020). The median, 5th, and 95th percentile values from the HyRAM+ leak frequency distributions are provided in Table 2; these values are included in the analysis to provide a range of comparisons, since the leak frequency data has uncertainties and built-in assumptions.

The second and third conditions considered were high shear wave velocity (V_{S30} of 760 m/s) and low shear wave velocity (160 m/s) seismic conditions, which were presented in Table 1 as the Frequency of Total Pipe Failure per Year per Meter. These annual leak frequencies solely attributed to seismic activity are also provided in Table 2 for comparison. These numbers show the comparison between the magnitudes of pipe leak frequencies under seismic conditions compared.

Table 2. Annual leak frequencies per meter of pipe for normal, non-seismic-specific as well as seismic conditions, assuming a pipe median ground acceleration capacity (\hat{A}) of 1.1 g. Percentages refer to leak sizes based on the percentage of the cross-sectional area of the pipe. * = Data not available.

	Annual Leak Frequency (leaks/year)				
	0.01%	0.1%	1%	10%	100%
Normal, non-seismic-specific conditions (5th percentile)	2.49×10^{-6}	1.15×10^{-6}	1.21×10^{-7}	6.41×10^{-8}	7.06×10^{-9}
Normal, non-seismic-specific conditions (median)	8.02×10^{-6}	3.70×10^{-6}	9.56×10^{-7}	4.61×10^{-7}	1.47×10^{-7}
Normal, non-seismic-specific conditions (95th percentile)	2.59×10^{-5}	1.17×10^{-5}	7.57×10^{-6}	3.13×10^{-6}	2.84×10^{-6}
Slow shear wave velocity seismic conditions ($V_{S30} = 160$ m/s)	*	*	*	*	7.1×10^{-9}
Fast shear wave velocity seismic conditions ($V_{S30} = 760$ m/s)	*	*	*	*	2.87×10^{-9}

When compared to the leak frequencies under seismic conditions, the median annual leak frequencies under normal, non-seismic-specific conditions are around one order of magnitude greater for $V_{S30} = 160$ m/s and around two orders of magnitude greater for $V_{S30} = 760$ m/s. The annual leak frequencies per meter of pipe under seismic conditions ($V_{S30} = 160$ or 760 m/s) are most similar to the leak frequencies under the 5th percentile normal (non-seismic-specific) conditions. There is a 95% chance that the leak frequency value will be higher than the 5th percentile value; median values are potentially more useful as a measure of central tendency.

Non-seismic specific risks as well as seismic risks were calculated separately (i.e., the leak frequencies from each row in Table 2 were used for each risk calculation). The resulting risk contours are shown in Figure 5. The normal, non-seismic-specific risk contours on the top show the normal, everyday risk derived from HyRAM+ data (Ehrhart et al. 2023), while the seismic risk contours only include seismic risk.

The contour plots provide some indication of how considering seismic risk could impact overall and annual individual risk. First, as expected, the magnitude of risk follows the trends of the leak frequencies. For normal, non-seismic-specific risk, the 5th percentile values are optimistic estimates of low leak frequencies while the 95th percentile values show conservative estimates of higher leak frequencies. For seismic conditions, the risk under $V_{S30} = 160$ m/s land conditions is higher than the risk for $V_{S30} = 760$ m/s, which is expected because $V_{S30} = 160$ m/s corresponds to softer soil and higher likelihood of ground motion which can lead to pipe rupture.

The annual individual risk for each condition, based on the person's distance in front of the leak, is shown in Figure 6. The same data is tabulated in Table A-2 in the Appendix A for reference.

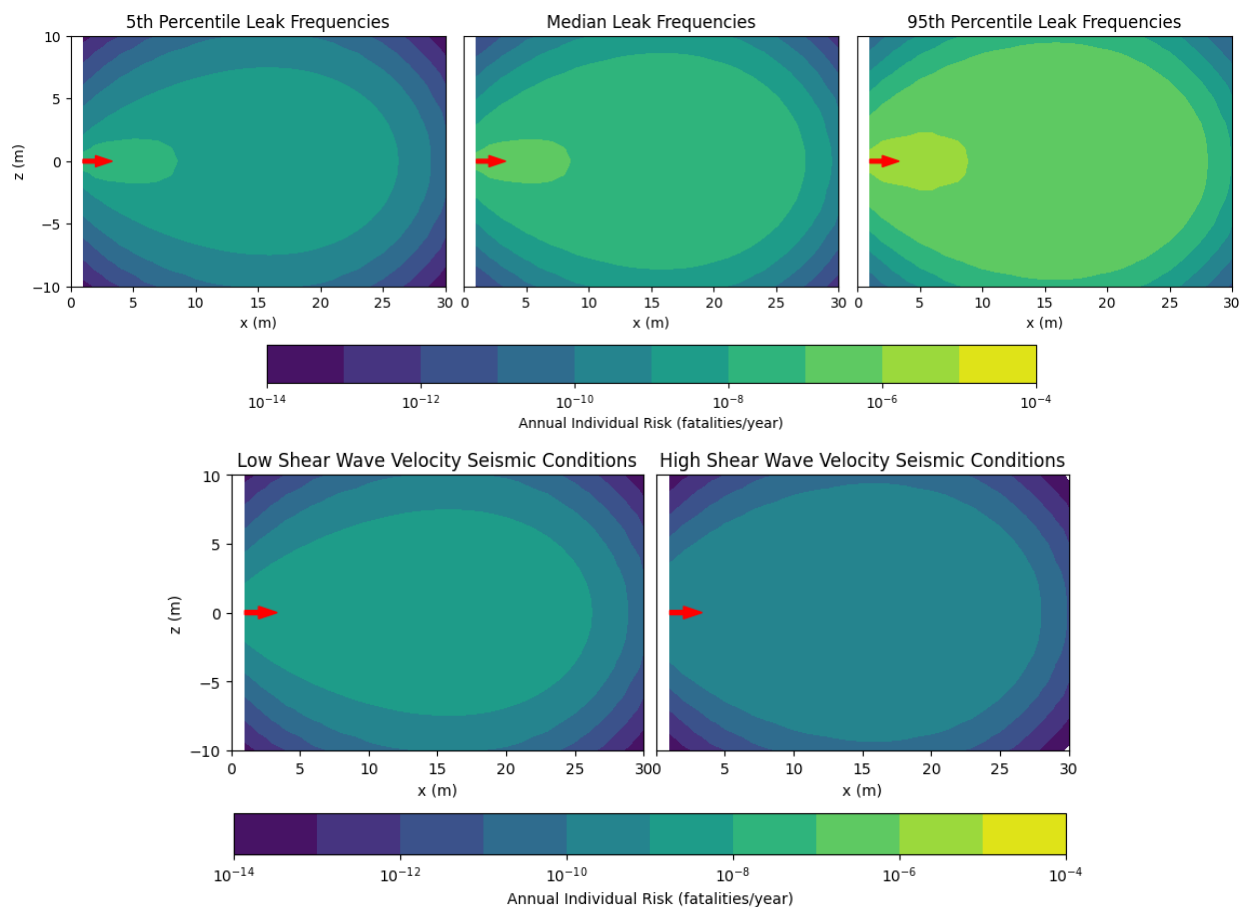


Figure 5. Two-dimensional contour plot of annual individual risks (birds-eye view) for full bore leaks. The red arrow indicates the leak origin and direction; it is not indicative of the size of the leak. Top: 5th, median, and 95th percentile leak frequency distributions for normal, non-seismic-specific conditions. Bottom left: $V_{S30} = 160$ m/s seismic conditions. Bottom right: $V_{S30} = 760$ m/s seismic conditions.

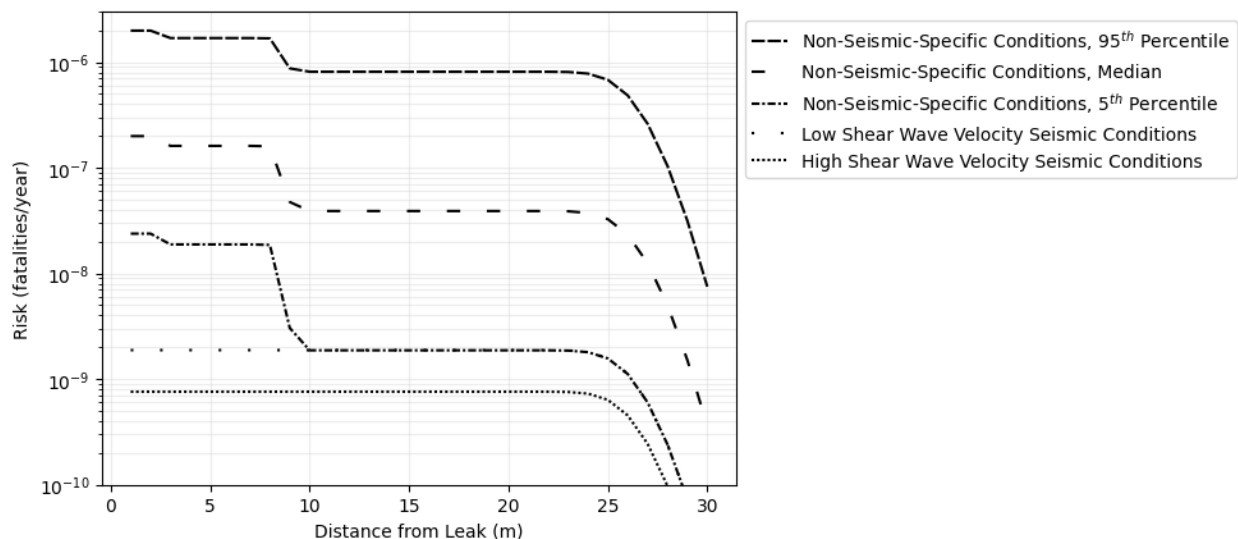


Figure 6. Annual individual risk for full bore leaks based on distance from the leak.

Figure 6 shows that for the conservative 95th percentile leak frequency risk values (which are under normal, non-seismic-specific conditions), the annual individual risk is around three orders of magnitude larger than the risk for higher shear wave velocity ($V_{s30} = 760$ m/s) seismic conditions and around two orders of magnitude larger compared to lower shear wave velocity ($V_{s30} = 160$ m/s) seismic conditions. Near the source of the leak, the median annual individual risk under normal, non-seismic-specific conditions is over two orders of magnitude greater than the risk values for higher shear wave velocity seismic conditions and around two orders of magnitude larger compared to lower shear wave velocity seismic conditions values. These differences suggest that while seismic risk should not be ignored, it is not as significant as the risk under normal non-seismic conditions for full-bore leaks. Though seismic fatality risk is not as significant compared to the risk considering normal, non-seismic-specific conditions, these results show that soil conditions may affect seismic risk values to some degree.

As was observed when comparing leak frequency data, individual risk values are around the same order of magnitude when the seismic conditions values are compared to those for the 5th percentile leak frequency values under normal, non-seismic-specific conditions. Because the consequences for all cases are the same, differences in risk are directly due to differences in likelihood. For the 5th percentile leak frequency values and those under seismic conditions, there is little difference between individual fatality risk particularly at distances 10 m and farther from the leak. As was the case for leak frequency comparisons, the 5th percentile risk values under normal non-seismic-specific conditions are associated with lower leak frequencies and lower fatality rates compared to the median and are therefore considered optimistic and an underestimate of risk.

One of the main reasons the estimated risk under seismic conditions is considerably lower than the risk under normal, non-seismic-specific conditions is because the annual individual risk under seismic conditions, though potentially catastrophic, is associated with conditions that occur very infrequently. The risk under normal non-seismic-specific conditions considers a breadth of everyday conditions, including normal use, maintenance, as well as possibly anomalous environmental situations such as earthquakes and other geophysical or meteorological stressors. Hence, risk data such as leak frequencies and fatality rates under normal non-seismic-specific conditions also consider seismic conditions to some degree. Performing the analysis shown in this work can help elucidate the contribution of elements such

as seismic conditions on the overall risk, especially if other contributions to risk can be isolated and quantified.

As discussed, this risk assessment only includes pipes, due to lack of available seismic data for other components; it also only includes full-bore leaks and excludes all partial leak sizes. Thus, while the results somewhat show overall trends of seismic risk compared to overall risk, the actual risk for the entire system may be different, since seismic conditions may affect components in various ways, and smaller leaks under both seismic and non-seismic-specific conditions may impact the overall risk through their varying leak frequencies and potential consequences in ways that cannot be predicted without more data. The method of mounting or connecting a component, and its natural frequency, are both considerations that may impact the frequency of various leak sizes of different components.

4.0 Possible Mitigation Approaches

Risk mitigation strategies in design and operation can be used to reduce leak frequencies and risk in regions susceptible to seismic activities. Regarding design, the piping network materials, placement, and orientation can be selected such that the pipes experience as little compression as possible and have the ability to elastically deform under tension (Nair & Dash, 2015). A thorough understanding of the characteristics of the regional and seismic activity around the facility would be needed for this pipe alignment. Additionally, using pipes with thick walls, anchoring and welding pipes for seismic conditions, designing a piping network with mostly straight sections and few sharp angles, and minimizing the buried depth of the pipeline (if it is underground and buried) can also help reduce leaks in the system during seismic events (Nair & Dash, 2015). Remediation of ground conditions in and around the piping network trench also may be beneficial; for example, some studies have suggested that lining sloped trench walls with geosynthetic materials or adding material to the trench to reduce liquefaction and lateral spreading of soil during seismic events may also improve the resilience of an underground pipe network (Nair & Dash, 2015).

Operationally, documented procedures for regular pipe network inspections, maintenance, repair, and replacement can ensure that the piping network remains updated and resilient to seismic effects. Protocol development and documentation for emergency response at the facility in the case of seismic activity and potential pipe leakage is also imperative for risk reduction. For example, the use of shutoff valves or an emergency shutdown system could help reduce the likelihood of hydrogen releases and subsequent ignition events, although accurate earthquake prediction is not currently possible, and even early earthquake warning occurs after a seismic event has already started.

5.0 Conclusion

Because Oregon has a significant risk of experiencing a major earthquake in the next 50 years, and PDX may serve as a key response center for Oregon during a seismic event, quantifying risks associated with such an event may be valuable in helping decision-making that will enable uninterrupted operation. This analysis provides risk assessment results under normal operations as well as seismic (CSZ earthquake) conditions for a hypothetical on-site hydrogen refueling station which would serve a hypothetical fleet of fuel cell electric buses. We present an analysis of these risks associated with pressurized hydrogen piping, the probability of a full-bore pipe leak, annual fatality risk due to such a rupture, and potential mitigation strategies to enhance resilience. This report serves as a resource for informing decision-makers and stakeholders about some of the normal operational, as well as seismic, risks associated with hydrogen deployment and some of the interventions that can mitigate these risks.

We conducted a quantitative risk assessment to characterize the potential consequences of hydrogen pipe failures during seismic events for a hypothetical refueling facility. This work does not provide a comprehensive quantitative risk assessment for the entire refueling facility under seismic conditions but instead focuses on quantifying the risks of hydrogen pipe rupture, largely because of the relevant impact of pressurized flammable gas pipe rupture on risk and because of the availability of seismic risk data for pipes carrying pressurized hydrogen. Pipe fragility data were taken from NUREG/CR-5759 and applied with the exceedance hazard curve to estimate pipe failure frequency under seismic conditions. To calculate the pipe failure frequency under normal, non-seismic-specific conditions, leak frequency data from HyRAM+ v5.1.1 were used. HyRAM+ also was used to determine the magnitude of consequences of ignition events under seismic and normal, non-seismic specific conditions. In this analysis, we quantified risk in terms of the individual annual frequency of fatality.

Risks were calculated under three different conditions:

1. Normal, non-seismic-specific conditions (5th, median, and 95th percentile leak frequencies for full-bore leaks (100% of the pipe cross-sectional area))
2. High shear wave velocity ($V_{S30} = 760$ m/s) full bore leaks under seismic conditions
3. Low shear wave velocity ($V_{S30} = 160$ m/s) full bore leaks under seismic conditions.

Normal, non-seismic-specific data are based on everyday leak activity of gaseous hydrogen components from generic oil and gas industry data. These data include leaks from different sources over time, potentially including leaks from seismic activity.

Softer soil conditions, such as near the Columbia River, are characterized by lower shear wave velocity and tend to amplify ground motions. The PDX site-specific seismic hazard assessment showed that the likelihood of full-bore pipe failure in hydrogen refueling systems is influenced by soil conditions; however, while soil conditions increase the probability of pipe rupture, the median risk of seismic pipe rupture for both softer (7.10×10^{-9} leaks/yr) or stiffer soil conditions (2.87×10^{-9} leaks/yr) are relatively small compared to the risk of pipe rupture under normal non-seismic specific conditions (1.47×10^{-7} leaks/yr).

Near the source of the leak, the annual individual risk (fatalities/yr) using median leak frequency values under normal, non-seismic-specific conditions is two orders of magnitude greater than the risk values for higher shear wave velocity ($V_{S30} = 760$ m/s) as well as lower shear wave

velocity seismic conditions. These differences suggest that, while seismic risk should not be ignored, it is not as significant as the risk under normal non-seismic conditions for full-bore leaks.

The reason for the estimated risk under seismic conditions being considerably lower than the risk under normal, non-seismic-specific conditions is twofold. First, the annual individual risk under seismic conditions, though potentially catastrophic, is associated with conditions that occur very infrequently, and second, the risk under normal non-seismic-specific conditions considers a breadth of activities and environmental circumstances, including those that might be anomalous such as earthquakes.

To enhance the resilience of hydrogen infrastructure at PDX, several mitigation strategies have been proposed. From a design perspective, the selection of materials, pipe placement, and orientation can be optimized to minimize the risk of leaks during seismic events. Employing pipes with thicker walls, using proper anchoring and welding systems, designing straight piping networks with minimal sharp angles, and reinforcing trench walls may reduce the likelihood of failure. Operationally, the establishment of comprehensive inspection and maintenance protocols, establishing documented emergency response procedures if leaks occur, and training staff on these protocols also can mitigate risk, ultimately contributing to the safety and functional continuity of services at PDX.

6.0 References

- Nair, G.S., Dash, S.R. and Matsagar, V. (2015). Review of seismic mitigation techniques for buried pipelines in fault zones. In *Structural Engineering Convention* (pp. 2794-2810). Zurich, Switzerland: International Association for Bridge and Structural Engineering (IABSE).
- Ehrhart, B., E. Hecht, and B. Schroeder. 2023. *Hydrogen Plus Other Alternative Fuels Risk Assessment Models (HyRAM+) Version 5.1 Technical Reference Manual*. Sandia National Laboratories. SAND--2023-14224. Albuquerque, NM. <https://doi.org/10.2172/2369637>.
- Glover, A. M., D. M. Brooks, and A. R. Baird. 2020. *Hydrogen Plant Hazards and Risk Analysis Supporting Hydrogen Plant Siting near Nuclear Power Plants (Final Report)*. Sandia National Laboratories. SAND--2020-10828. Albuquerque, NM. <https://doi.org/10.2172/1678837>.
- Goldfinger, C., C. H. Nelson, J. E. Johnson, and S. S. Party. 2003. "Holocene Earthquake Records from the Cascadia Subduction Zone and Northern San Andreas Fault Based on Precise Dating of Offshore Turbidites." *Annual Review of Earth and Planetary Sciences* 31 (1): 555-577.
- R. P. Kennedy, "Risk based seismic design criteria," Nuclear engineering and design, vol. 192, no. 2-3, pp. 117-135, 1999.
- Louie, M., M. Miletic, and B. Ehrhart. n.d. *Quantitative Risk Assessment for Fuel Cell Electric Bus Hydrogen Storage and Refueling Facility*. Sandia National Laboratories. (Publication in Progress).
- McPhillips, D. F., J. A. Herrick, S. Ahdi, A. K. Yong, and S. Haefner. 2020. Updated Compilation of V_{S30} Data for the United States. U.S. Geological Survey data release. <https://earthquake.usgs.gov/data/vs30/us/>.
- Multnomah County. 2023. "NHMP Final Draft - Chapter 5 - Jurisdictional/District Profiles, Section 5.7, Port of Portland." In *Natural Hazards Mitigation Planning*. Portland, OR: Multnomah County, Oregon. https://multco.us/file/nhmp_final_draft_section_5.7_port_of_portland/download.
- NIBS. 2021. *Portland International Airport (PDX) Resilient Runway Benefit-Cost Analysis*. National Institute of Building Sciences. Washington, D.C. https://nibs.org/wp-content/uploads/2025/04/NIBS_PDX_Resilient_Runway_Benefit-Cost_Analysis_Report-1.pdf.
- NRC. 1993. *Risk Analysis of Highly Combustible Gas Storage, Supply, and Distribution Systems in Pwr Plants*. U.S. Nuclear Regulatory Commission. NUREG/CR-5759. Washington, D.C.
- Petersen, M. D., A. M. Shumway, P. M. Powers, E. H. Field, M. P. Moschetti, K. S. Jaiswal, K. R. Milner, S. Rezaeian, A. D. Frankel, and A. L. Llenos. 2024. "The 2023 US 50-State National Seismic Hazard Model: Overview and Implications." *Earthquake Spectra* 40 (1): 5-88.
- Simion, G. P., et al. Risk analysis of highly combustible gas storage, supply, and distribution systems in PWR Plants. No. NUREG/CR-5759; EGG-2640. Nuclear Regulatory Commission,

Washington, DC (United States). Div. of Safety Issue Resolution; EG and G Idaho, Inc., Idaho Falls, ID (United States), 1993.

USGS. 2018a. USGS Earthquake Hazard Toolbox: Disaggregation, NSHM Conterminus U.S. 2018. U.S. Geological Survey.

https://earthquake.usgs.gov/nshmp/hazard/disagg?commonReturnPeriods=2475&latitude=NaN&longitude=NaN&maxDirection=false&model=CONUS_2018&returnPeriod=2475&siteClass=BC&truncate=false&disaggComponent=Total&disaggTarget=RETURN_PERIOD&iml=null&imt=PGA&vs30=760.

USGS. 2018b. USGS Earthquake Hazard Toolbox: Dynamic Hazard Curves, NSHM Conterminus U.S. 2018. U.S. Geological Survey.

https://earthquake.usgs.gov/nshmp/hazard/dynamic?commonReturnPeriods=2475&latitude=NaN&longitude=NaN&maxDirection=false&model=CONUS_2018&returnPeriod=2475&siteClass=BC&truncate=false&imt=PGA&sourceType=Total&vs30=760.

Appendix A – Supplemental Data

Table A-1. Input parameters for quantitative risk assessment.

Risk Assessment Category	Risk Assessment Input	Value
Physical Parameters		
Component Specification	Pipe Inner Diameter	7.9375 mm (5/16")
Fuel Conditions	Fuel Temperature	-40°C (-40°F)
	Fuel Pressure	7×10^4 kPa (10,153 psi)
Ambient Conditions	Ambient Temperature	20°C (68°F)
	Ambient Pressure	101.326 kPa (14.7 psi)
	Relative Humidity	89%
	BST Flame Speed	Mach 0.35
Leak Conditions	Discharge Coefficient	1
Qualitative Risk Assessment Parameters		
Occupant Parameters	Working Time	2000 hours
Leak Detection Parameters	Probability of Leak Detection and Isolation	90%
Ignition Parameters	Ignition Probabilities	Release Rate Ignition Probability
		(kg/s) Immediate Delayed
		<0.125 0.008 0.004
		0.125–6.25 0.053 0.027
		>6.25 0.230 0.120
	Jet Fire Exposure Time	30 seconds
Probits	Overpressure Computation Method	Baker-Strehlow-Tang (BST)
	Thermal Probit Model	Eisenberg
	Overpressure Probit Model	TNO Head Trauma

Table A-2. Annual individual risk based on distance from the leak, using 50 pipes for normal, non-seismic-specific and seismic conditions.

Distance from Leak (m)	Normal, non-Seismic-Specific Conditions (5th Percentile)	Normal, Non-Seismic-Specific Conditions (Median)	Normal, Nonseismic-Specific Conditions (95th Percentile)	Risk Associated With Fast Shear Wave Velocity Seismic Conditions ($V_{S30} = 760$ m/s)	Risk Associated With Slow Shear Wave Velocity Seismic Conditions ($V_{S30} = 160$ m/s)
1	2.38×10^{-8}	1.99×10^{-7}	1.99×10^{-6}	7.60×10^{-10}	1.88×10^{-9}
2	2.38×10^{-8}	1.99×10^{-7}	1.99×10^{-6}	7.60×10^{-10}	1.88×10^{-9}
3	1.88×10^{-8}	1.61×10^{-7}	1.69×10^{-6}	7.60×10^{-10}	1.88×10^{-9}
4	1.88×10^{-8}	1.61×10^{-7}	1.69×10^{-6}	7.60×10^{-10}	1.88×10^{-9}
5	1.88×10^{-8}	1.61×10^{-7}	1.69×10^{-6}	7.60×10^{-10}	1.88×10^{-9}
6	1.88×10^{-8}	1.61×10^{-7}	1.69×10^{-6}	7.60×10^{-10}	1.88×10^{-9}
7	1.88×10^{-8}	1.61×10^{-7}	1.69×10^{-6}	7.60×10^{-10}	1.88×10^{-9}
8	1.86×10^{-8}	1.60×10^{-7}	1.68×10^{-6}	7.60×10^{-10}	1.88×10^{-9}
9	3.05×10^{-9}	4.73×10^{-8}	8.72×10^{-7}	7.60×10^{-10}	1.88×10^{-9}
10	1.87×10^{-9}	3.89×10^{-8}	8.11×10^{-7}	7.60×10^{-10}	1.88×10^{-9}

Distance from Leak (m)	Normal, non- Seismic- Specific Conditions (5th Percentile)	Normal, Non- Seismic-Specific Conditions (Median)	Normal, Nonseismic- Specific Conditions (95th Percentile)	Risk Associated With Fast Shear Wave Velocity Seismic Conditions ($V_{S30} = 760$ m/s)	Risk Associated With Slow Shear Wave Velocity Seismic Conditions ($V_{S30} = 160$ m/s)
11	1.87×10^{-9}	3.89×10^{-8}	8.11×10^{-7}	7.60×10^{-10}	1.88×10^{-9}
12	1.87×10^{-9}	3.89×10^{-8}	8.11×10^{-7}	7.60×10^{-10}	1.88×10^{-9}
13	1.87×10^{-9}	3.89×10^{-8}	8.11×10^{-7}	7.60×10^{-10}	1.88×10^{-9}
14	1.87×10^{-9}	3.89×10^{-8}	8.11×10^{-7}	7.60×10^{-10}	1.88×10^{-9}
15	1.87×10^{-9}	3.89×10^{-8}	8.11×10^{-7}	7.60×10^{-10}	1.88×10^{-9}
16	1.87×10^{-9}	3.89×10^{-8}	8.11×10^{-7}	7.60×10^{-10}	1.88×10^{-9}
17	1.87×10^{-9}	3.89×10^{-8}	8.11×10^{-7}	7.60×10^{-10}	1.88×10^{-9}
18	1.87×10^{-9}	3.89×10^{-8}	8.11×10^{-7}	7.60×10^{-10}	1.88×10^{-9}
19	1.87×10^{-9}	3.89×10^{-8}	8.11×10^{-7}	7.60×10^{-10}	1.88×10^{-9}
20	1.87×10^{-9}	3.89×10^{-8}	8.11×10^{-7}	7.60×10^{-10}	1.88×10^{-9}
21	1.87×10^{-9}	3.89×10^{-8}	8.11×10^{-7}	7.60×10^{-10}	1.88×10^{-9}
22	1.87×10^{-9}	3.88×10^{-8}	8.11×10^{-7}	7.59×10^{-10}	1.88×10^{-9}
23	1.86×10^{-9}	3.86×10^{-8}	8.06×10^{-7}	7.55×10^{-10}	1.87×10^{-9}
24	1.80×10^{-9}	3.73×10^{-8}	7.79×10^{-7}	7.30×10^{-10}	1.81×10^{-9}
25	1.57×10^{-9}	3.26×10^{-8}	6.80×10^{-7}	6.37×10^{-10}	1.58×10^{-9}
26	1.12×10^{-9}	2.32×10^{-8}	4.84×10^{-7}	4.53×10^{-10}	1.12×10^{-9}
27	6.02×10^{-10}	1.25×10^{-8}	2.61×10^{-7}	2.44×10^{-10}	6.05×10^{-10}
28	2.40×10^{-10}	4.99×10^{-9}	1.04×10^{-7}	9.75×10^{-11}	2.42×10^{-10}
29	7.27×10^{-11}	1.51×10^{-9}	3.15×10^{-8}	2.95×10^{-11}	7.30×10^{-11}
30	1.73×10^{-11}	3.59×10^{-10}	7.50×10^{-9}	7.03×10^{-12}	1.74×10^{-11}

Pacific Northwest National Laboratory

902 Battelle Boulevard
P.O. Box 999
Richland, WA 99354

1-888-375-PNNL (7665)

www.pnnl.gov